Microporous and Mesoporous Materials 348 (2023) 112395

Contents lists available at ScienceDirect

Microporous and Mesoporous Materials

journal homepage: www.elsevier.com/locate/micromeso

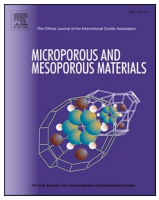

Optical study of oriented double-Se_8-ring clusters and luminescent Se_2^- anions in LTA at extremely high selenium loading density

Vladimir V. Poborchii [a,*], Vitalii P. Petranovskii [b], Igor A. Glukhov [c,d], Andrei A. Fotiadi [e]

[a] National Institute of Advanced Industrial Science and Technology, Tsukuba, 305-8565, Japan
[b] Centro de Nanociencias y Nanotecnología, Universidad Nacional Autónoma de México, Ensenada, Baja California, Mexico
[c] Lab-STICC (UMR CNRS 6285), École Nationale d'Ingénieurs de Brest, France
[d] Ulyanovsk State University, 42 Leo Tolstoy Street, Ulyanovsk, 432970, Russia
[e] Optoelectronics and Measurement Techniques unit, University of Oulu, Oulu, Finland

ARTICLE INFO

Keywords:
Zeolite single crystals
Selenium
Raman/Brillouin microscopy
Photoluminescence

ABSTRACT

Recently, LTA-Se(1–8) samples with 1–8 Se atoms per cavity (simplified unit cell, large cavity + sodalite cage) obtained via adsorption at the temperature of ~450 °C were reported. It was shown that single Se_8 or single Se_{12} ring are formed in the large LTA cavities, Se_8/Se_{12} ring concentration ratio decreasing with an increase in the Se loading density. Contrary, in the present work, using Se vapour adsorption at ~550 °C, we succeeded in encapsulation of ~17 Se atoms per cavity (LTA-Se(17)) with a significant increase in the Se_8/Se_{12} concentration ratio manifesting double Se_8-ring cluster formation in the most of the LTA large cavities, which is a step towards cluster crystal fabrication. According to our polarization/orientation Raman spectroscopic study of LTA-Se(17) single crystals, the orientations of the Se_8 and Se_{12} appeared to be similar to those in previously investigated LTA-Se(1–8). Importantly, luminescent Se_2^- anions, oriented along the LTA 4-fold axes and located in the sodalite cages, are detected via Raman polarization/orientation dependencies of LTA-Se(17). Bright Se_2^- light emission with a maximum at ~1.56 eV and vibronic structure is observed in the 1.3–1.8 eV spectral range. We show that the anions experience a compression in LTA which is slightly relaxing with a decrease in temperature producing an anomalous Raman band downshift. The compression of Se_2^- in LTA is weaker/stronger than that in sodalite/cancrinite, luminescence band photon energy depending on its strength. High concentration of regularly arranged Se_2^- in LTA suggests considering LTA-Se(17) as an important novel light-emitting material.

1. Introduction

Selenium is considered as an important material since the 19th century due to its photosensitivity [1] and, especially, from the mid-20th century due to its applications in xerography [2]. In the 21st century, Se and its compounds are employed in solar-energy devices [3], topological-insulator materials [4], lithium batteries [5] etc. A few years ago, Se nanoparticles were explored as anti-microbial/cancer/oxidant agents and tunable light-emitting bio-markers [6–8]. Zeolites themselves are important alumino-silicate materials with uniform sub-nanometer scale pores enabling molecular hosting and exhibiting unique chemical, optical and elastic properties [9–11]. Formation of LTA-based functional materials with a resonance electronic inter-cluster interaction at high loading densities is another important point. Therefore, LTA zeolite with regularly arranged highly-concentrated Se particles is attractive subject for research nowadays.

Here, we focus on the optical properties of Se species confined and regularly arranged in the ~1.14 nm size large cavities and ~0.63 nm size sodalite cages of the LTA zeolite. Using Se vapour adsorption at the temperature t ~550 °C, we succeeded in encapsulation of ~17 Se atoms per simplified unit cell (large cavity + sodalite cage), which is significantly higher than the Se loading densities obtained in our previous works, where adsorption was done at t ~ 450 °C [12–15]. In those works, we were able to univocally identify Raman and optical absorption bands of previously unknown Se_{12} rings. However, in order to make a step towards fabrication of a new functional material with the interacting Se clusters, we need to increase Se loading density, which is achieved in the present work. Polarized Raman spectra (RS) of so-prepared LTA-with-Se single crystals (LTA-Se(17)) show that the most of Se is stabilized in the form of double-Se_8-ring clusters in the LTA

* Corresponding author.
E-mail address: Vladimir.Poborchii@gmail.com (V.V. Poborchii).

https://doi.org/10.1016/j.micromeso.2022.112395
Received 7 October 2022; Received in revised form 27 November 2022; Accepted 6 December 2022
Available online 7 December 2022

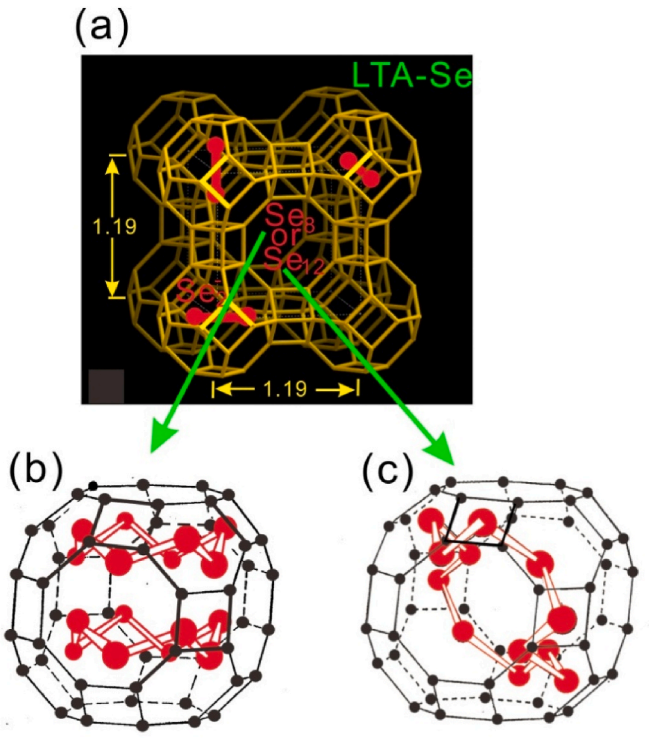

Fig. 1. Framework of LTA (a); Se_8 double ring cluster (b) and Se_{12} (c) schematic view in the LTA large cavity. Se_2^- anions are shown in the sodalite cages (a).

large cavities, with the rest of the large cavities being occupied by single Se_{12} rings. Importantly, luminescent Se_2^- anions appeared to be formed in the LTA sodalite cages at t ~550 °C. The anions experience a compression in LTA which is slightly relaxing with a decrease in temperature producing an anomalous Raman band downshift, luminescence band photon energy depending on its strength. Their high concentration and regular arrangement suggests considering LTA-Se(17) as a promising light-emitting material. We should stress that our polarization/orientation Raman technique allows studying relatively small LTA single crystals compared to the size of >40 μm required for X-ray diffraction (XRD). Another advantage of our technique is a possibility of identifying types and orientations of a variety of molecules in the same crystal, which is difficult for XRD due to partial occupancies of Se atom sites. Additionally, we have to note that such periodically arranged system of Se clusters and light-emitting centers could be an interesting system for high-spatial-resolution luminescence and Raman/Brillouin imaging techniques.

2. Experimental

Synthetic LTA zeolites ($Na_{12}Al_{12}Si_{12}O_{48}$) were used in this work. LTA has nearly spherical-shape large cavities with diameter of ~1.14 nm which are connected through narrow windows of ~0.42 nm diameter (Fig. 1). Each large cavity is accompanied by a small cavity, sodalite cage, with the diameter of ~0.63 nm. The zeolite structures are accessible at the International Zeolite Association website http://www.iza-structure.org/IZA-SC/ftc_table.php. The sizes of the cubic LTA crystals were ~20 μm along the edge of the cube. Dehydration of zeolites in vacuum was performed in pyrex ampoules at t ~550 °C. The selenium vapour adsorption was done at the same temperature during a week. Amount of adsorbed Se was determined via an accurate zeolite powder and selenium weighing before the adsorption and then controlled with the LTA-Se density measurement using single crystal flotation in Clerici solutions [16].

RS were studied using Renishaw micro-Raman spectrometer with ~1 μm focused laser probe size. The 514.5 nm line of the Ar^+ laser and 785 nm line of the infrared light-emitting-diode laser were used for the RS excitation. Photo-luminescence spectra excited with the 514.5 nm line were recorded using the same spectrometer. Optical absorption spectra (OAS) in the visible and near UV spectral ranges were studied using Carl Zeiss and CRAIC micro-optical spectrometers, the light probe size being <10 μm. The samples were intentionally broken to minimize their optical density and placed into glycerol between two cover glasses to avoid surface light scattering.

3. Double Se_8 ring clusters in LTA-Se(17): a step towards a cluster crystal

At the Se adsorption temperature of ~550 °C, we succeeded in significant increase in the Se loading density in LTA-Se up to ~ 17 at./cav. (here cavity (cav.) means the simplified unit cell). No sign of the zeolite water was observed in RS and IR spectra of so-prepared LTA-Se(17). Formally, the obtained loading density of ~17 at./cav. roughly corresponds to two Se_8 rings per cavity. However, our spectroscopic data show that the situation is more complicated. At first, we have found that in addition to the Se ring molecules, Se_2^- anions are formed in the LTA-Se (17) (we discuss the Se_2^- anions in the following section). At second, still significant amount of Se_{12} rings is found in this sample like in LTA-Se prepared at t ~450 °C [12–15].

Fig. 2(a) shows RS of LTA-Se(17) for different polarization configurations (first/second index stands for the polarization of incident/scattered light) at the 785 nm excitation wavelength. Spectra for LTA-Se(8) from Ref. [13] are shown in Fig. 2(b). In contrast with the tendency observed for the increase of Se loading density from 1 to 8 at./cav. showing a gradual decrease in the Se_8/Se_{12} Raman band intensity ratio [13], the increase from 8 to 17 at./cav. clearly shows an increase in the Se_8/Se_{12} band intensity ratio Fig. 2(a and b). This fact is an argument for

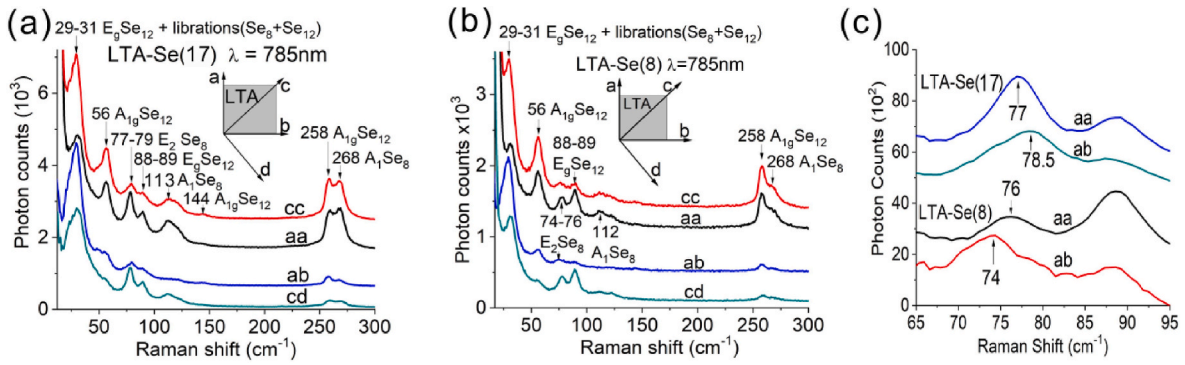

Fig. 2. Raman spectra of LTA-Se(17) (a), LTA-Se(8) (b) for **cc**-, **aa**-, **ab**- and **cd**-polarization configurations at the 785 nm excitation wavelength with the axis directions shown in the insets; Se_8 E_2 mode band splitting for both samples (c).

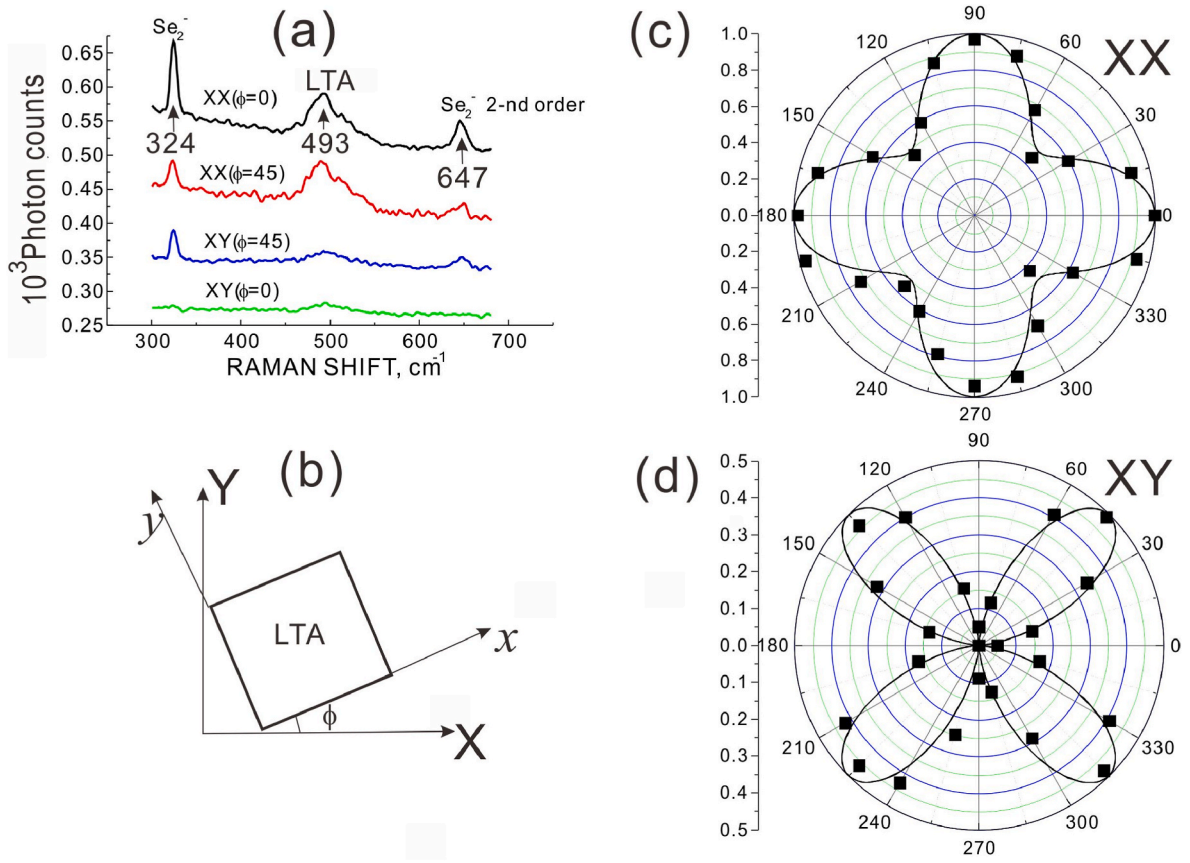

Fig. 3. Raman spectra of Se_2^- in LTA-Se(17) for different polarization configurations at the 514.5 nm excitation wavelength (a); schematic view of the LTA-Se(17) crystal rotated in the laboratory co-ordinate XY-plane (b); polarization/orientation dependencies of the Se_2^- band intensity on the angle φ for XX (c) and XY (d) polarization configurations, lines standing for theoretical calculations and squares representing experimental points.

the double Se_8 ring formation in the large LTA cavities. Taking into account an approximate Se_8/Se_{12} concentration ratio of ~3.5 at the 8 at./cav. Se loading density [13] and the observed here a factor of ~2.3 increase in the Se_8/Se_{12} RS band intensity ratio in LTA-Se(17), compared to LTA-Se(8), we conclude that ~20% of the cavities are occupied with Se_{12} while the rest of the large cavities are filled with the double Se_8 rings. Also taking into account Se_2^- anions, which are, probably, located in nearly every sodalite cage, we obtain ~17 at./cav. in agreement with the experimental Se-loading-density value.

RS polarization dependencies in Fig. 2(a and b) are similar to each other. Therefore, the ring orientations in both samples are like those reported earlier for LTA-Se(8) [13,15] with the only difference that LTA-Se(17) has two Se_8 rings in the large cavity (Fig. 1(b)) while LTA-Se (8) has only one Se_8 [13]. The Se_{12} ring orientation is shown in Fig. 1(c).

In the restricted space of the LTA large cavity, two Se_8 rings are slightly compressed compared to a single Se_8 ring. One can see a confirmation for this in RS of LTA-Se(17). Indeed, the A_1 symmetric bond-bending mode band of a double Se_8 ring cluster in LTA-Se(17) at ~113 cm^{-1} displays an upshift compared to ~112 cm^{-1} for a single Se_8 in LTA-Se(8). Both values are smaller than ~114 cm^{-1} of the Se_8 ring in AFI-Se indicating rather strong compression of the ring in the 0,73 nm wide AFI channel [13].

An interesting change is observed for the E_2 bond-bending mode that is split off due to a zeolite-induced reduction of the Se_8 ring D_{4d} symmetry (Fig. 2(c)). The E_2 bond bending mode band of the double ring cluster displays both upshift and reverse split off compared to that of the single Se_8 ring. For a single Se_8 ring in LTA-Se(8), the **aa**-active component displays frequency of ~76 cm^{-1} which is higher than that of the **ab**-active component of ~74 cm^{-1}. However, for a doublle Se_8 ring cluster in LTA-Se(17), the **aa**-active component displays frequency of ~77 cm^{-1} which is lower than that of the **ab**-active component at ~78.5 cm^{-1}. Probably, a single Se_8 ring LTA-Se(8) is rather centrally located in the cavity while the Se_8 location in LTA-Se(17) is more peripheral. Therefore, the symmetry distortion of the ring is different in these two cases. Anyway, our data definitely suggest that the dihedral and bond angles of double Se_8 rings are decreased compared to a single Se_8 ring to make the double rings more compact.

Turning back to the basic ideas of the cluster crystal fabrication [17–19], we stress that making a regular lattice of clusters in LTA is very important. The cluster crystal requirement includes uniformity of the cavity-confined clusters and their electron-resonance interaction. Compared to single Se_8/Se_{12} ring formation in LTA-Se(8) [13], the double Se_8-ring fabrication in the most of the LTA cavities is a big step towards this goal.

4. Raman, optical absorption and luminescence spectra of Se_2^- in LTA-Se(17): its compression and anomalous temperature dependence of the vibration frequency

RS of Se_2^- formed in LTA-Se(17) taken with the 514.5 nm wavelength laser are shown in Fig. 3(a) for four polarization configurations. (φ is the angle between the laboratory **X**-axis and the crystal [100] ***x***-axis (Fig. 3 (b).) The 1st-order Raman band of Se_2^- is displayed at ~324 cm^{-1} and the 2nd-order one at ~647 cm^{-1}. The observed 1st-order frequency is close to the frequencies observed for the same anion in other zeolites such as SOD-Se (331-334 cm^{-1}) [20], CAN-Se (320 cm^{-1}) [21] and Nd-FAU-Se (328 cm^{-1}) [22], the frequencies being dependent on the interaction with zeolites. Taking into account the fact that the Se_2^- is Raman active at the 514.5 nm excitation only when both incident and scattered lights are polarized along the molecule axis [21], the LTA-Se

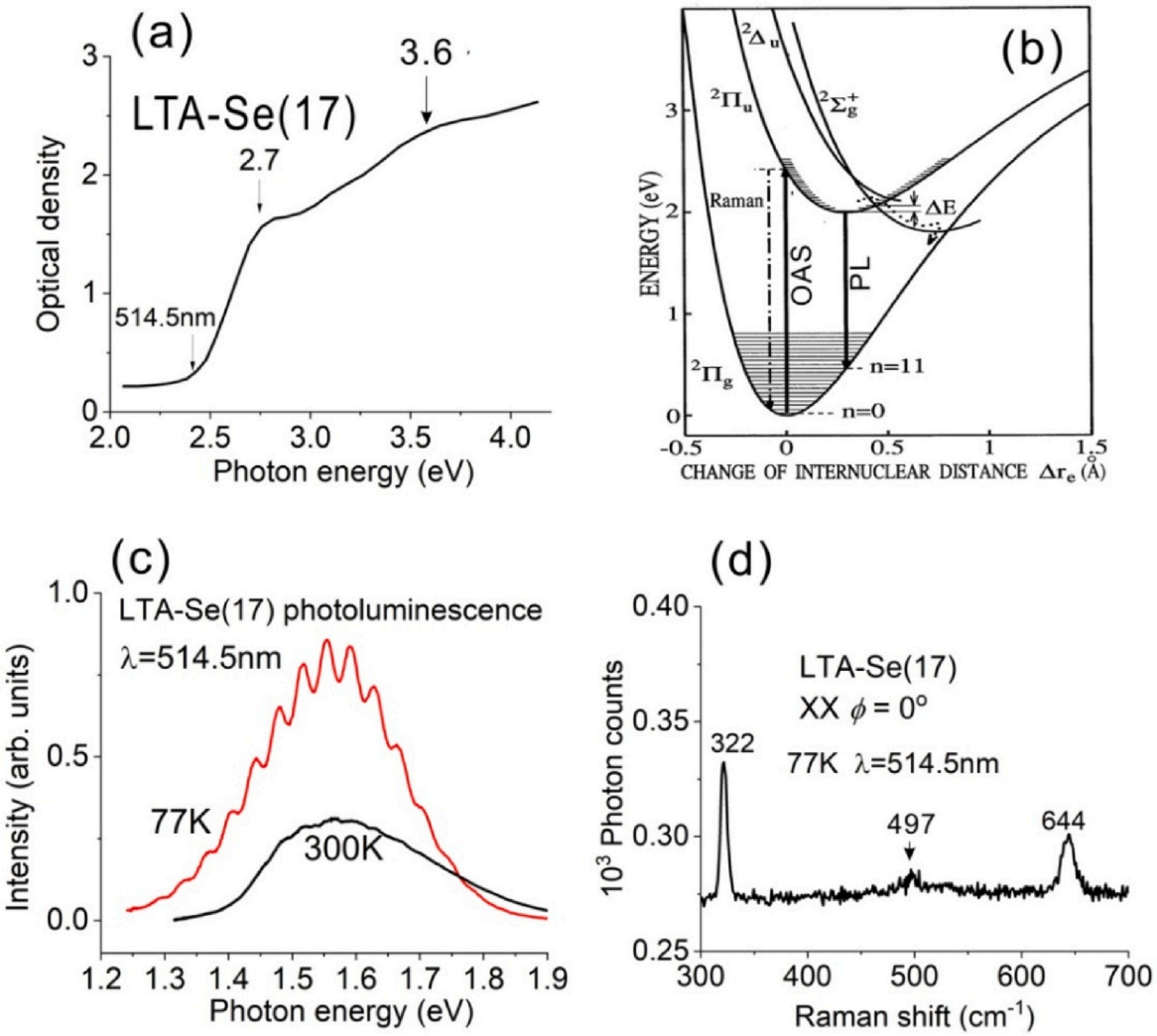

Fig. 4. Room temperature OAS of LTA-Se(17) (a); Se_2^- electron structure [26] with schematically shown absorption (OAS) and luminescence (PL) transitions (b); LTA-Se(17) PL spectra at the temperatures of ~300 K (black) and ~77 K (red) (c); RS of LTA-Se(17) at ~77 K. (For interpretation of the references to colour in this figure legend, the reader is referred to the Web version of this article.)

(17) polarization dependence clearly shows that the Se_2^- anions are oriented along the 4-fold axes of LTA crystals. Small size and negative charge of the species suggest that they are, probably, located in sodilite cages of LTA (Fig. 1(a)) like S_3^- [23]. Interestingly, in case of CAN-Se, luminescent Se_2^- are formed when Se or Na_2Se_4 was added to initial components used for the synthesis of cancrinite [18]. Contrary, only Se_2^{2-} are formed in CAN-Se obtained via Se vapour adsorption [24,25].

Importantly, Se_2^- is a very suitable example of the polarization-orientation dependencies of RS intensity of a linear molecule located in a cubic crystal. Fig. 3 shows such dependencies for the **XX**(c) and **XY** (d) polarization configurations vs. the angle φ between the **X**-direction of the laboratory system of co-ordinates and the ***x***-axis of the LTA crystal (Fig. 3(b)). Using the method [16] based on a general formula for RS efficiency of vibrations, we can easily find that the contribution of Se_2^- oriented along the ***x***- and ***y***-axis to the **XX**-configuration RS displays $\cos^4(\varphi)$ and $\sin^4(\varphi)$ dependencies, respectively. Summation gives us $\sin^4(\varphi)+\cos^4(\varphi)$ dependence clearly reproduced experimentally in Fig. 3 (c). For the **XY**-configuration, both ***x***-oriented and ***y***-oriented molecules contribute like $\sin^2(\varphi)\cos^2(\varphi)$ in good agreement with the experiment shown in Fig. 3(d), The Se_2^- bands completely vanish in the **XY**-configuration at $\varphi = 0^0$ (Fig. 4(a,d)), which confirms the perfect dimer orientation along the 4-fold axis of LTA.

OAS measurement of LTA-Se(17) was rather difficult due to the high absorption of the sample. Even ~0.1 μm thick pieces of LTA-Se(17) crystals showed very high optical densities. Typical OAS of LTA-Se (17) is shown in Fig. 4(a). The Se_2^- band at ~2.7 eV due to the $^2\Pi_g \rightarrow {}^2\Pi_u$ electron transition [20,26] (Fig. 4(b)) strongly contributes to the spectrum. The Se_{12} and Se_8 rings mainly contribute to the absorption at the photon energies >3 eV [13]. The absorption peak at ~3.6 eV belongs to the double Se_8 ring cluster, the energy being slightly lower than that of single Se_8 at 3.75–3.85 eV [13].

It is known that the Se_2^- anions display bright photo-luminescence (PL) in the red–near-infrared spectral range [20]. Steady-state PL spectra of LTA-Se(17) excited with the 514.5 nm light at the temperatures of ~300 K and ~77 K are shown in Fig. 4(c). A broad luminescence band with a maximum at ~1.56 eV and a distinct vibronic structure is displayed in the LTA-Se(17) PL spectrum taken at ~77 K. The band is related to the $^2\Pi_u \rightarrow {}^2\Pi_g$ electron transition like that in SOD-Se [20], reverse to the absorption electron transition between the same molecular electronic states. The Se loading density of ~17 at./cav. suggests that the anions occupy nearly every sodalite cage. Otherwise, we need to admit that some additional optically invisible Se species are formed in LTA-Se. As we mentioned above, no Se_2^- was formed at the adsorption temperature of ~450 °C [13]. Probably, higher concentration of Se_2 molecules in Se vapour and larger amplitude of sodalite-cage-window vibrations at ~550 °C play a crucial role in the encapsulation of Se_2 in

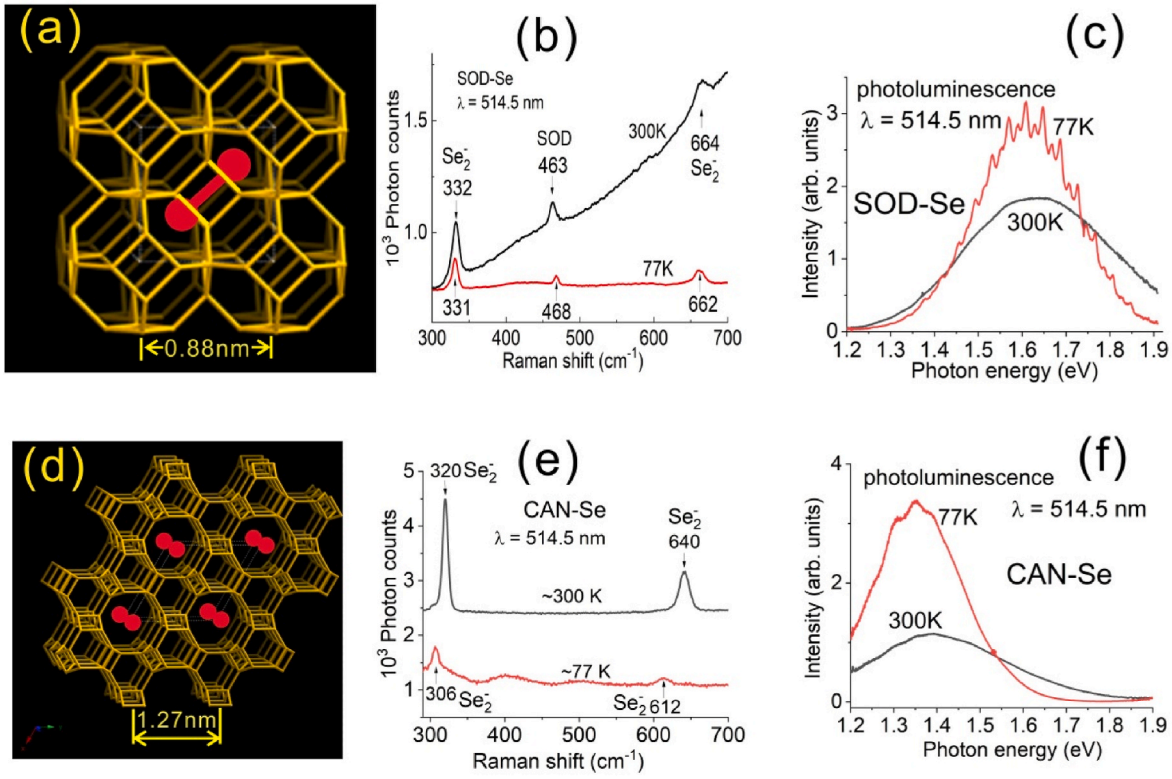

Fig. 5. Schematic view of Se_2^- in SOD-Se with the molecule orientation proposed in Ref. [20] (a); RS of SOD-Se at the temperatures of ~300 K (black) and ~77 K (red) (b); PL spectra of SOD-Se at the temperatures of ~300 K (black) and ~77 K (red) (c); schematic view of Se_2^- in CAN-Se (d); RS of SOD-Se at the temperatures of ~300 K (black) and ~77 K (red) for incident and scattered lights polarized along CAN channels (e); PL spectra of CAN-Se at the temperatures of ~300 K (black) and ~77 K (red) (f). (For interpretation of the references to colour in this figure legend, the reader is referred to the Web version of this article.)

sodalite cages. A neutral Se_2 molecule, after occupation of the sodalite cage borrows an electron from the zeolite framework. Theoretically, we can place Se_2^- in the window between two large cavities with the orientation along the 4-fold axis. This would be beneficial for the interaction of the clusters in the large cavities, which is important for the cluster crystal. However, Se_2^- location in the sodalite cage looks more reasonable.

Fig. 4(d) shows RS of LTA-Se(17) taken at the temperature of ~77 K, other conditions being equal to those of RS in Fig. 3(a), black curve. Surprisingly, instead of the expected Raman upshift with a decrease in temperature (like the LTA band does), the Se_2^- band displays a noticeable downshift from 324 cm^{-1} to ~322 cm^{-1}. This can be explained by the anion compression at ~300 K and its partial relaxation at ~77 K. It is confirmed by the significant enhancement of the Se_2^- Raman intensity compared to that of the zeolite one with a decrease in temperature. According to the Se_2^- electronic structure, an increase in the anion's interatomic distance causes a decrease in the electron energy gap between the $^2\Pi_g$ and $^2\Pi_u$ states and red shift of the Se_2^- absorption band. Therefore, the resonance Raman condition should be improved at the 514.5 nm excitation when the Se_2^- absorption band positioned at ~2.7 eV at ~300 K is downshifted at ~77 K.

Let us focus on the environment influence on the Se_2^- properties in other zeolites. Fig. 5 shows positions, RS and PL spectra of Se_2^- in SOD-Se with ~0.63 nm diameter pores and CAN-Se with ~0.6 nm diameter channels. The room-temperature vibration frequency increase from ~320 cm^{-1} in CAN-Se (Fig. 5(e)) to ~332 cm^{-1} in SOD-Se (Fig. 5(b)) suggests a quite strong compression of Se_2^- anions in SOD. Indeed, Se_2^- is confined only in two dimensions in the CAN channels and it is not confined in the anion axis direction (Fig. 5(d)). Contrary, Se_2^- is confined in all three dimensions in the cages of SOD (Fig. 5(a)). Correspondingly, the frequency of ~320 cm^{-1} of the anion in CAN-Se indicates its larger inter-atomic distance than that in the compressed one in SOD-Se with the frequency of ~332 cm^{-1}. Se_2^- in LTA-Se(17) displays an intermediate frequency of ~324 cm^{-1} (Fig. 3(a)) corresponding to a relatively slight compression of the anion in the sodalite cage of LTA. The photon energy positions of the Se_2^- luminescence bands in three zeolites (Figs. 4(c) and 5(c,f)) appear to be in agreement with the compression effect on the anion's electronic structure (Table 1).

Table 1
Raman and photo-luminescence peak positions of Se_2^- anion formed in cancrinite, LTA and sodalite.

Se_2^-	CAN	LTA	SOD
frequency (cm^{-1}) at 300/77 K	320/306	324/322	332/331
PL peak (eV) at 300/77 K	1.39/1.35	1.57/1.56	1.63/1.62

Temperature dependence of Se_2^- RS in SOD-Se (Fig. 5(b)) is similar to that in LTA-Se(17), namely, its frequency of ~331 cm^{-1} at ~77 K is lower than ~332 cm^{-1} at ~300 K. Contrary, the sodalite band frequency of ~468 cm^{-1}at ~77 K is higher than ~463 cm^{-1} at ~300 K in accordance with regular temperature-induced expansion/contraction. Temperature dependence of Se_2^- RS in CAN-Se (Fig. 5(e)) suggests effect of combining of two or more Se_2^- molecules into chain at low temperatures [21].

Probably, Na^+ cations play important role in a strong Se_2^- compression in SOD-Se. Orientation of the anion surrounded with three Na^+ cations along the 3 fold axis of SOD (Fig. 5(a)) was proposed in Ref. [20]. Contrary, as we found via the polarization/orientation RS, LTA-confined Se_2^- are oriented along the 4-fold axis of the zeolite. The sodalite cage space in this direction is slightly larger than that in the 3-fold axis one implying less compression of the anion. The cation sites in LTA-Se(17) are, probably, same as those in dehydrated LTA mainly in the windows between the large cavity and sodalite cage [27] and a few other sites out of the cage leaving more space for Se_2^- in it than that in SOD-Se.

In CAN-Se, the cations located near the channel walls make nearly no impact on Se_2^- aligned in the center of the channel along its direction (Fig. 5(d)). As pointed out in Ref. [20], the stress around Se_2^- does not allow growing large SOD-Se crystals with a significant concentration of the anions. Contrary, it is not an obstacle in LTA, which is beneficial for LTA-Se(17) as a light-emitting material. Thus, the anion compression depends on several parameters, namely: the pore size, the anion orientation and the cation influence. The anomalous temperature dependence of its Raman shift is an important scientific discovery related to the adsorbed material properties.

5. Conclusions

Using Se vapour adsorption at ~550 °C, we succeeded in encapsulation of ~17 Se atoms per unit cell of the LTA zeolite single crystals. By means of the polarized Raman spectroscopy of so-prepared LTA-Se(17), we demonstrate formation of mainly double-Se_8-ring clusters with a minor quantity of single Se_{12} rings in the large LTA cavities. ~80% of the large cavities are filled with Se_8 while the rest ~20% with Se_{12}. Despite quite long history of studies of LTA-Se fabricated by different methods (high-pressure Se melt injection [28] and vapour adsorption at different temperatures [12–15,29–33]), this work provides the first clear evidence for the double-Se_8-ring-cluster formation. Slightly compressed luminescent Se_2^- anions, oriented along the LTA 4-fold axes and located in the sodalite cages, are detected via Raman polarization/orientation dependencies of LTA-Se(17), the compression being partially relaxed with a decrease in temperature producing an anomalous Se_2^- Raman downshift. Our conclusion about the formation of Se rings in the LTA large cavities and diatomic Se species in the sodalite cages is, basically, in agreement with the LTA-Se 85-micron-size single crystal XRD data [33]. Bright Se_2^- light emission with a maximum at ~1.56 eV and vibronic structure is observed in the 1.3–1.8 eV spectral range. The compression of Se_2^- in LTA is weaker/stronger than that in sodalite/-cancrinite, luminescence band photon energy depending on its strength. High concentration of regularly arranged Se_2^- emission centers suggests considering LTA-Se(17) as an important novel light-emitting material. Moreover, the obtained LTA-Se(17) crystal could be an extremely interesting system for testing high-spatial-resolution luminescence, Raman and even Brillouin imaging techniques.

CRediT authorship contribution statement

Vladimir V. Poborchii: Writing – review & editing, Writing – original draft, Visualization, Validation, Supervision, Resources, Project administration, Methodology, Investigation, Formal analysis, Data curation, Conceptualization. **Vitalii P. Petranovskii:** Validation, Resources, Methodology, Conceptualization. **Igor A. Glukhov:** Visualization, Software, Formal analysis. **Andrei A. Fotiadi:** Validation, Methodology, Funding acquisition, Formal analysis.

Declaration of competing interest

The authors declare that they have no known competing financial interests or personal relationships that could have appeared to influence the work reported in this paper.

Data availability

Data will be made available on request.

Acknowledgment

We thank G.-G. Lindner for SOD-Se and CAN-Se samples containing Se_2^-. I.A.G. kindly acknowledges for the support from Ministry of Science and Higher Education of the Russian Federation (075-15-2021-581). A. A.F. is supported by the European Union's Horizon 2020 research and innovation programme (H2020-MSCA–IF–2020, #101028712).

References

[1] W. Smith, Effect of light on selenium during the passage of electric current, Nature 7 (1873) 303, https://doi.org/10.1038/007303e0.
[2] S.B. Berger, R.C. Enck, M.E. Scharfe, B.E. Springett, The application of selenium and its alloys to xerography, in: E. Gerlach, P. Grosse (Eds.), The Physics of Selenium and Tellurium vol. **13**, Springer Series in Solid-State Sciences, Springer, Berlin, Heidelberg, 1979, pp. 256–266, https://doi.org/10.1007/978-3-642-81398-6_40.
[3] I. Hadar, T.-B. Song, W. Ke, M.G. Kanatzidis, Modern processing and insights on selenium solar cells: the world's first photovoltaic device, Adv. Energy Mater. (2019), 1802766, https://doi.org/10.1002/aenm.201802766.
[4] H. Zhang, C.-X. Liu, X.-L. Qi, X. Dai, Z. Fang, S.-C. Zhang, Topological insulators in Bi_2Se_3, Bi_2Te_3 and Sb_2Te_3 with a single Dirac cone on the surface, Nat. Phys. **5** (2009) 438–442, https://doi.org/10.1038/nphys1270.
[5] T.C. Mendes, C. Nguyen, A.J. Barlow, P. Cherepanov, M. Forsyth, P.C. Howlett, D. R. MacFarlane, A safe Li-Se battery in an ionic liquid-based electrolyte operating at 25-70 °C by using a N,S,O tri-doped mesoporous carbon host material, Sustain. Energy Fuel. 4 (2020), https://doi.org/10.1039/C9SE01074B.
[6] J. Mal, W.J. Veneman, Y.V. Nancharaiah, E.D. van Hullebusch, W.J.G. M. Peijnenburg, M.G. Vijver, P.N.L. Lens, A comparison of fate and toxicity of selenite, biogenically and chemically synthesized selenium nanoparticles to zebrafish (Danio rerio) embryogenesis, Nanotoxicology 11 (2017) 87–97, https://doi.org/10.1080/17435390.2016.1275866.
[7] A. Khalid, P.A. Tran, R. Norello, D.A. Simpson, A.J. O'Connor, S. Tomljenovic-Hanic, Intrinsic fluorescence of selenium nanoparticles for cellular imaging applications, Nanoscale 8 (2016) 3376–3385, https://doi.org/10.1039/c5nr08771f.
[8] E. Piacenza, A. Presentato, B. Heyne, R.J. Turner, Tunable photoluminescence properties of selenium nanoparticles: biogenic versus chemogenic synthesis, Nanophotonics 9 (2020) 3615–3628, https://doi.org/10.1515/nanoph-2020-0239.
[9] M.I.M. Alzeer, H. Nguyen, T. Fabritius, H. Sreenivasan, V.-V. Telkki, A.M. Kantola, C. Cheeseman, M. Illikainen, P. Kinnunen, On the hydration of synthetic aluminosilicate glass as a sole cement precursor, Cement Concr. Res. 159 (2022), 106859, https://doi.org/10.1016/j.cemconres.2022.106859, 2022.
[10] X. Lan, J. Huang, Q. Han, T. Wei, Z. Gao, H. Jiang, J. Dong, H. Xiao, Fiber ring laser interrogated zeolite-coated singlemode-multimode-singlemode structure for trace chemical detection, Opt Lett. 37 (2012) 1998, https://doi.org/10.1364/ol.37.001998.
[11] C. Sanchez-Valle, S.V. Sinogeikin, Z.A.D. Lethbridge, R.I. Walton, C.W. Smith, K. E. Evans, J.D. Bass, Brillouin scattering study on the single-crystal elastic properties of natrolite and analcime zeolites, J. Appl. Phys. 98 (2005), 053508, https://doi.org/10.1063/1.2014932.
[12] V.V. Poborchii, M.S. Ivanova, V.P. Petranovskii, Y.A. Barnakov, A. Kasuya, Y. Nishina, Raman and absorption spectra of the zeolites A and X containing selenium and tellurium in the nanopores, Mater. Sci. Eng. 217/218 (1996) 129–134, https://doi.org/10.1016/S0921-5093(96)10365-8.
[13] V.V. Poborchii, A.V. Fokin, Raman and optical absorption spectra of oriented Se_8 and Se_{12} rings formed in zeolites: dependence on the Se loading density, Microporous Mesoporous Mater. 338 (2022), 111954, https://doi.org/10.1016/j.micromeso.2022.111954.
[14] V.V. Poborchii, Raman spectra of sulfur, selenium or tellurium clusters confined in nano-cavities of zeolite A, Solid State Commun. 107 (1998) 513–518, https://doi.org/10.1016/S0038-1098(98)00205-1.
[15] V.V. Poborchii, Raman microprobe polarization measurements as a tool for studying the structure and orientation of molecules and clusters incorporated into cubic zeolites: S_8 and Se_{12} rings in zeolite A, J. Chem. Phys. 114 (2001) 2707–2717, https://doi.org/10.1063/1.1339268.
[16] R.H. Jahns, Clerici solution for the specific gravity determination of small mineral grains, Am. Mineral. 24 (1939) 116–122.
[17] V.N. Bogomolov, Liquids in ultrathin channels (Filament and cluster crystals), Sov. Phys. Usp. **21** (1978) 77–83, https://doi.org/10.1070/PU1978v021n01ABEH005510.
[18] G.D. Stucky, J.E. MacDougall, Quantum confinement and host/guest chemistry: probing a new dimension, Science 247 (1990) 669–678, https://doi.org/10.1126/science.247.4943.669.
[19] G.A. Ozin, Synthesis in diminishing dimensions, Adv. Mater. 4 (1992) 612–649, https://doi.org/10.1002/adma.19920041003.
[20] H. Schlaich, G.-G. Lindner, J. Feldmann, E.O. Go1bel, D. Reinen, Optical properties of Se2- and Se2 color centers in the red selenium ultramarine with the sodalite structure, Inorg. Chem. 39 (2000) 2740–2746.
[21] V.V. Poborchii, G.-G. Lindner, M. Sato, Selenium dimers and linear chains in one-dimensional cancrinite nanochannels: structure, dynamics, and optical properties, J. Chem. Phys. 116 (2002) 2609–2617, https://doi.org/10.1063/1.1434950.
[22] A. Goldbach, M. Grimsditch, L. Iton, M.-L. Saboungi, Photoinduced Formation of selenium molecules in zeolites: a resonant Raman spectroscopy study, J. Phys. Chem. B 101 (1997) 330–334, https://doi.org/10.1021/jp962563w.
[23] V.N. Bogomolov, V.P. Petranovskii, V.V. Poborchii, S.V. Kholodkevich, Absorption, Raman and ESR spectra and the dielectric permittivity of NaA-S cluster crystals, Sov. Phys. Solid State 25 (1983) 1415–1417.
[24] V.N. Bogomolov, A.N. Efimov, M.S. Ivanova, V.V. Poborchii, S.G. Romanov, Y. I. Smolin, Y.F. Shepelev, Structure and optical properties of a one-dimensional

chain of selenium atoms in a cancrinite channel, Sov. Phys. Solid State 34 (1992) 916–919.
[25] V.V. Poborchii, M. Sato, A.V. Shchukarev, Linear dimerized Se chains in cancrinite nanochannels: x-ray diffraction and photoelectron spectra, Solid State Commun. 103 (1997) 649–654, https://doi.org/10.1016/S0038-1098(97)00272-X.
[26] H. Murata, T. Kishigami, R. Kato, Time-resolved study of photoluminescence from Se_2^- molecule in KI, J. Phys. Soc. Jap 59 (1990) 506–515, https://doi.org/10.1143/JPSJ.59.506.
[27] R.Y. Yamagida, A.A. Amaro, K. Seff, Redetermination of the crystal structure of dehydrated zeolite 4A, J. Phys. Chem. 77 (1973) 805–809, https://doi.org/10.1021/j100625a014.
[28] V.N. Bogomolov, E.L. Lutsenko, V.P. Petranovskii, S.V. Kholodkevich, Absorption spectra of three-dimensionally-ordered system of 12 Å particles, JETP Lett. 23 (1976) 482–484.
[29] V.N. Bogomolov, V.V. Poborchii, S.V. Kholodkevich, S.I. Shagin, Electronic and vibrational spectra of 10-Å selenium clusters; cluster model of amorphous selenium, JETP Lett. 38 (1983) 532–535.
[30] V.N. Bogomolov, V.V. Poborchii, S.V. Kholodkevich, Size effects in the vibrational spectrum of 10-Å selenium particles, JETP Lett. 42 (1985) 517–520.
[31] J.B. Parise, J.E. MacDougal1, N. Herron, R. Farlee, A.W. Sleight, Y. Wang, T. Bein, K. Moiler, L.M. Moroney, Characterization of Se-loaded molecular sieves A, X, AlPO-5 and mordenite, Inorg. Chem. 27 (1988) 221–228, https://doi.org/10.1021/ic00275a002.
[32] Y. Nozue, T. Kodaira, 0 Terasaki, K. Yamazakii, T. Goto, D. Watanabe, J. M. Thomas, Absorption spectra of selenium clusters and chains incorporated into zeolites, J. Phys. Condens. Matter 2 (1990) 5209–5217, https://doi.org/10.1088/0953-8984/2/23/011.
[33] H.S. Kim, J.S. Park, W.T. Lim, Structural study of selenium sorption complex of fully dehydrated, partially Ca^{2+}-exchanged zeolite A, Korean J. Mineral. Petrol. 33 (2020) 251–258, https://doi.org/10.22807/KJMP.2020.33.3.251.